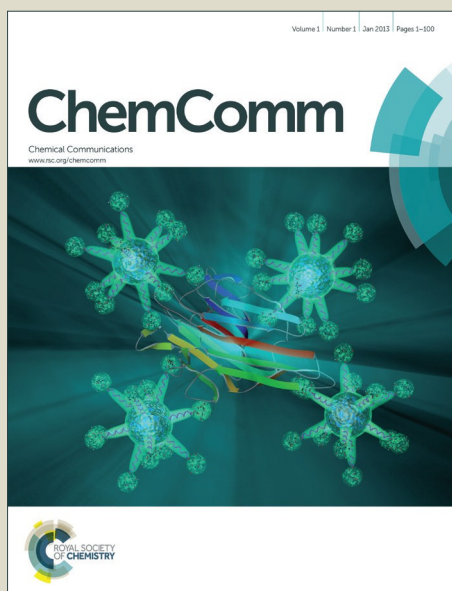


# ChemComm

Accepted Manuscript



This article can be cited before page numbers have been issued, to do this please use: L. Zhang, L. Han, G. Zhao, R. Chai, Q. Zhang, Y. Liu and Y. Lu, *Chem. Commun.*, 2015, DOI: 10.1039/C5CC03009A.



This is an *Accepted Manuscript*, which has been through the Royal Society of Chemistry peer review process and has been accepted for publication.

*Accepted Manuscripts* are published online shortly after acceptance, before technical editing, formatting and proof reading. Using this free service, authors can make their results available to the community, in citable form, before we publish the edited article. We will replace this *Accepted Manuscript* with the edited and formatted *Advance Article* as soon as it is available.

You can find more information about *Accepted Manuscripts* in the [Information for Authors](#).

Please note that technical editing may introduce minor changes to the text and/or graphics, which may alter content. The journal's standard [Terms & Conditions](#) and the [Ethical guidelines](#) still apply. In no event shall the Royal Society of Chemistry be held responsible for any errors or omissions in this *Accepted Manuscript* or any consequences arising from the use of any information it contains.

Cite this: DOI: 10.1039/c0xx00000x

www.rsc.org/xxxxxx

ARTICLE TYPE

## Structured Pd-Au/Cu-fiber catalyst for gas-phase hydrogenolysis of dimethyl oxalate to ethylene glycol

Li Zhang,<sup>‡</sup> Lupeng Han,<sup>‡</sup> Guofeng Zhao,<sup>\*</sup> Ruijuan Chai, Qiaofei Zhang, Ye Liu, and Yong Lu<sup>\*</sup>

Received (in XXX, XXX) Xth XXXXXXXXX 20XX, Accepted Xth XXXXXXXXX 20XX

DOI: 10.1039/b000000x

**Galvanic co-deposition of 0.5 wt% Au and 0.1 wt% Pd on a microfibrillar-structure using 8- $\mu$ m Cu-fiber delivers a Pd-Au/Cu-fiber catalyst, being highly active, selective and stable for hydrogenolysis of dimethyl oxalate to ethylene glycol. Au and Pd synergistically promote the hydrogenolysis activity of Cu<sup>+</sup> sites while Au also critically stabilize Cu<sup>+</sup> sites to prevent deep reduction deactivation.**

Green and sustainable production of chemicals and fuels based on C1 chemistry via syngas (mixture of CO and H<sub>2</sub>) from abundant various carbon sources (such as biomass, natural gas, coal and even municipal solid waste) is an amazing alternative to the petrochemical-based production.<sup>1-3</sup> Particularly, ethylene glycol (EG) is a versatilely-used commodity chemical in various applications, such as antifreeze, solvents, and the manufactures of heats transfer agents, polymer, and many other chemical products.<sup>2,4</sup> The current commercial production of EG is mainly depending on the hydrolysis of petroleum-based ethylene oxide.<sup>4</sup> However, along with the petroleum dwindling there is an increasingly severe dilemma between the constantly increased price of petroleum and demand for EG. Therefore, the C1-route synthesis of EG from syngas attracts more and more attentions, which could be realized through a two-step process consisting of the coupling of CO with nitrite esters to form dimethyl oxalate (DMO) and the subsequent hydrogenolysis of DMO to EG.<sup>5,6</sup>

The DMO hydrogenolysis has been considerably investigated in both liquid-phase and gas-phase. Ruthenium-based homogeneous catalysts were previously used for liquid-phase DMO hydrogenolysis with a high EG yield under milder conditions (95% at 7 MPa and 100 °C), but greatly suffered from the problems of corrosion and separation.<sup>7</sup> From the standpoint of industry, the gas-phase process is more attractive because of the convenience of catalyst separation and higher production efficiency especially for the EG production in a bulk form. The CuCr catalyst is reported to be highly active and selective in gas-phase DMO hydrogenolysis to EG, but the toxicity of Cr greatly hampers its application.<sup>8</sup> Subsequently, Cr-free Cu-based catalysts have been intensively investigated for this reaction. Different supports (e.g., SiO<sub>2</sub>, Al<sub>2</sub>O<sub>3</sub>, ZnO, and La<sub>2</sub>O<sub>3</sub>) for Cu-based catalysts are studied,<sup>9,10</sup> among which Cu/SiO<sub>2</sub> is considered to be the most active for the gas-phase DMO hydrogenolysis to EG, likely due to the neutral property of SiO<sub>2</sub>.<sup>11</sup> However, these oxides-supported Cu catalysts have inherent problems such as poor stability because of the

deterioration of active sites under real reaction conditions. Whereas the Cu/SiO<sub>2</sub> catalyst can highly actively and selectively convert DMO to EG, obvious deactivation is observed within 30 h due to the agglomeration of Cu species.<sup>12</sup> In order to improve the catalyst stability, boron-modified Cu/SiO<sub>2</sub> catalyst has been developed and its lifetime is dramatically prolonged to 300 hours under the identical reaction conditions.<sup>13</sup> In addition, AuCu/SBA-15 catalyst has also been reported to be effective for the hydrogenolysis of DMO to EG, with a prolonged lifetime of 240 h.<sup>14</sup> More recently, hydroxyapatite supported Cu catalyst is fabricated by a facile ammonia-assisted one-pot synthesis method for the hydrogenolysis of DMO to EG. It is reported that the lifetime of this catalyst is prolonged to 120 hours because of the stabilizing-effect of the phosphate species on the Cu particles and Cu<sup>+</sup> species.<sup>15</sup>

In the real world practice, however, the usage of silica support seems to be a fatal flaw due to its severe leaching caused by the reaction of SiO<sub>2</sub> with methanol in this reaction system,<sup>16</sup> which might be the main cause for low-quality rather than polymerization grade EG. Moreover, the DMO hydrogenolysis to EG is exothermic ( $\Delta H = -58.73 \text{ kJ mol}^{-1}$ ),<sup>17</sup> normally generating hotspots that is a main cause for catalyst sintering deactivation. Most current efforts have focused on improving the dispersion of Cu species or adding the promoters to alleviating their agglomeration,<sup>13-15,18</sup> but almost without any glance shot at enhancing catalyst heat-transfer ability. In fact, catalysts usually need to operate in adiabatic packed bed reactors with high conversion and in this case heat transfer effect cannot be overlooked. Hence, from both academic and industrial points of view, rendering a novel silica-free catalyst with unique combination of high activity and selectivity, structural robustness, and excellent thermal conductivity is particularly desirable.

Herein, we discover an efficient monolithic structured Pd-Au/Cu-fiber catalyst, obtainable by galvanically depositing Pd and Au nanoparticles (NPs) onto the fiber surfaces of thin-sheet microfibrillar structure prepared through wet layup paper making/sintering processes using 8- $\mu$ m Cu fibers with high heat conductivity.<sup>19</sup> The procedure for making this monolithic catalyst is schematically illustrated in Fig. 1a. Such galvanic deposition can proceed automatically when wetting the Cu-fiber surface with the aqueous solution containing appointed amount of Pd and Au cations, due to the large electrode potential differences between the Cu<sup>2+</sup>/Cu<sup>0</sup> (0.34 V) and Au<sup>3+</sup>/Au<sup>0</sup> (1.5 V; or Pd<sup>2+</sup>/Pd<sup>0</sup>, 0.95 V) pairs. A typical catalyst after calcination at 300 °C, 0.1Pd-

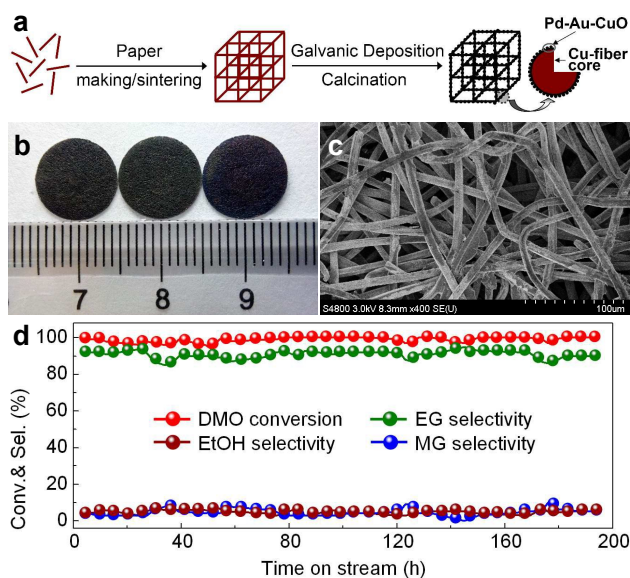


**Fig. 1** (a) Procedure for making the monolithic structured Pd-Au/Cu-fiber catalyst (Note: a cubic architecture here is used only to demonstrate the idea and the catalyst actually shows an irregular 3D structure as imaged by the posterior SEM). (b) Optical photograph and (c) SEM image of the 0.1Pd-0.5Au/Cu-fiber catalyst. (d) DMO conversion and products selectivities vs time on stream using 0.1Pd-0.5Au/Cu-fiber. Catalyst of 0.5 g, 13 wt% DMO dissolved in MeOH, WHSV of total liquid feed of 5.3 h<sup>-1</sup>, H<sub>2</sub> to DMO molar ratio of 180, 2.5 MPa, 270 °C.

**Table 1.** DMO hydrogenolysis over the various catalysts.

Catalyst	Conv. <sup>a</sup> (%)	Select. <sup>a,c</sup> (%)	TOF <sup>d</sup> (h <sup>-1</sup> )
0.1Pd-0.5Au/Cu-fiber <sup>b</sup>	99	93	612
Cu-fiber	40	1	17
0.1Pd/Cu-fiber <sup>b</sup>	98	85	80
0.5Au/Cu-fiber <sup>b</sup>	92	58	174

<sup>a</sup> Reaction conditions: 270 °C, 2.5 MPa, WHSV of total liquid feed of 5.3 h<sup>-1</sup> with 13 wt% DMO dissolved in MeOH, molar ratio of H<sub>2</sub> to DMO of 180. <sup>b</sup> Real loadings of Pd and Au, by ICP-AES, are shown in Table S2. <sup>c</sup> All the products include EG, MG and EtOH, and here only EG selectivity is shown with the detailed products selectivities shown in Table S3. <sup>d</sup> TOF: converted DMO molecules per surface Cu<sup>+</sup> site per hour, to see the calculation information and detailed results in Table S4 in ESI.

0.5Au/Cu-fiber, indicates a well-preserved thin-sheet microfibrillar structure (Fig. 1b), with characteristic irregular 3-dimension (3D) network (Fig. 1c). This catalyst is capable of converting 99% DMO, with the highest 93% selectivity to EG at 270 °C, as well as the selectivities to ethanol (EtOH) of 3% and methyl glycolate (MG, an important intermediate for the synthesis of pharmaceutical products and perfumes) of 4% for a feed of 13 wt% DMO dissolved in methanol (MeOH) with a total weight hourly space velocity (WHSV) of 5.3 h<sup>-1</sup> (Table 1, Fig. 1d). Particularly, the 0.1Pd-0.5Au/Cu-fiber is stable at least 200 h without any signs of deactivation (Fig. 1d). Tuning the Pd and Au loadings, including their contents and Au/Pd ratio, does not yield better performance than the 0.1Pd-0.5Au/Cu-fiber (Fig. S1). By comparison, our catalyst delivers slightly lower but comparable activity compared to the reported catalysts, and is more stable than the most reported ones even at higher reaction temperature (Table S1). Moreover, SiO<sub>2</sub>-free characteristics of our Cu-fiber-structured catalyst can avoid the reported Si-leaching problem.<sup>16</sup>

Extended studies on several other different Pd-Au catalyst

systems, including 0.1Pd-0.5Au/Al-fiber, 0.1Pd-0.5Au/SS-fiber (“SS” represents stainless-steel) and 0.1Pd-0.5Au/Ni-fiber, with 3D network (Fig. S2), size-distribution (Fig. S3) and loadings of Pd and Au similar to the 0.1Pd-0.5Au/Cu-fiber catalyst (Figs 1b,1c, Table S2), all yield very low DMO conversion of 7-10% for the hydrogenolysis of DMO under the identical reaction conditions (Table S3). This indicates that Pd and Au themselves deliver very poor activity for the titled reaction. In contrast, when placing Au and Pd together with Cu onto those microfibrillar structure using either Al-fiber, Ni-fiber or SS-fiber, DMO conversion is dramatically promoted to the level comparable to the Pd-Au/Cu-fiber catalyst with a total EG/MG selectivity of 98% (relatively more MG formation compared to the 0.1Pd-0.5Au/Cu-fiber; Table S3). In fact, the Cu-fiber pre-oxidized in air at 300 °C, with Cu<sub>2</sub>O phase formation (Fig. S4),<sup>20</sup> provides the crucial catalytic active sites of Cu<sup>+</sup> for the hydrogenolysis of DMO,<sup>2,13,21,22</sup> while leading to 40% DMO conversion under identical reaction conditions (Table 1). This conversion isn’t inconsiderable but much lower than that over the catalysts with the co-existence of Pd, Au and Cu<sup>+</sup> species. A possible explanation is that a special Pd-Au-Cu<sup>+</sup> ternary complex is formed with unique multi-synergistic effects, which is paramount to the enhanced activity/stability of the Pd-Au/Cu-fiber catalyst.

To reveal the multi-synergistic nature of such Pd-Au-Cu<sup>+</sup> ternary complex, experiments on turnover frequency (TOF, converted DMO per surface Cu<sup>+</sup> site per hour) measurements are firstly carried out at 210 °C by controlling DMO conversion below 30%, with the results collected in Table 1. Clearly, the pure Cu-fiber delivers a low but measurable TOF of 17 h<sup>-1</sup>. The single-introduction of Pd or Au into Cu-fiber could improve the TOF to 80 and 174 h<sup>-1</sup>, respectively, indicating the promotion-effect of Pd or Au on the catalyst activity (Table 1). Most notably, however, the 0.1Pd-0.5Au/Cu-fiber catalyst with co-introduction of Pd and Au could further enhance the TOF to 612 h<sup>-1</sup>, much higher than these over the 0.1Pd/Cu-fiber and 0.5Au/Cu-fiber catalysts (Table 1), indicating the synergistic-promotion-effect of Pd and Au on the catalyst activity. Subsequently, the stability testing is carried out over the pure Cu-fiber, 0.1Pd/Cu-fiber, and 0.5Au/Cu-fiber, with the results shown in Fig. S5. It is clearly demonstrated that the pure Cu-fiber delivers both a low DMO conversion and poor stability with a progressively decline of DMO conversion from 40% to 12% in 22 h (Fig. S5a). Interestingly, the 0.1Pd/Cu-fiber and 0.5Au/Cu-fiber catalysts both deliver high initial DMO conversion of 92-98% (Table 1), but 0.1Pd/Cu-fiber suffers from a fast decline of DMO conversion from 98% to 42% in 45 h, while the 0.5Au/Cu-fiber exhibits a much better stability with DMO converted stably in 90-92% throughout entire 80 h test (Figs S5b,5c), exhibiting the dual-effects of Au on both activity-promoting and stability-enhancing. More excitingly, the 0.1Pd-0.5Au/Cu-fiber catalyst could not only deliver a very high initial conversion of 99% but also greatly prolong the catalyst lifetime at such high conversion to at least 200 h without any signs of alternation in DMO conversion (Fig. 1d), indicating the synergistic-promotion-effect of Au-Pd on the catalyst activity and stability.

Considering the disparate TOFs and stability of the pure Cu-fiber, 0.1Pd/Cu-fiber, 0.5Au/Cu-fiber, and 0.1Pd-0.5Au/Cu-fiber under the identical reaction conditions, there should be different

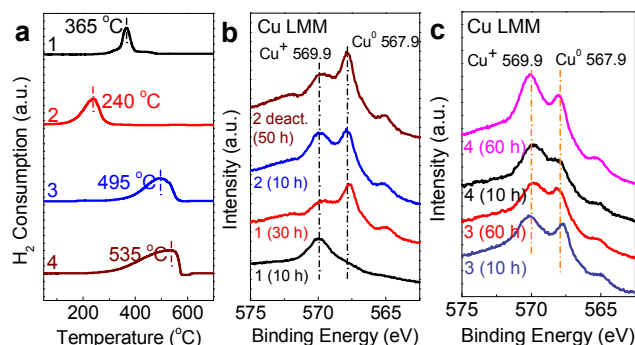


**Fig. 2** (a) TPR profiles of the catalysts. (b and c) Cu LMM Auger spectra of the samples at different reaction time for every catalyst. Sample 1: pure Cu-fiber; Sample 2: 0.1Pd/Cu-fiber; Sample 3: 0.5Au/Cu-fiber; Sample 4: 0.1Pd-0.5Au/Cu-fiber.

S4) is reduced at 365 °C (Fig. 2a), but the reduction of Cu<sub>2</sub>O over 0.1Pd/Cu-fiber (Fig. S4) takes place at much lower temperature of 240 °C (Fig. 2a), indicating that the Pd catalyzes the reduction of Cu<sub>2</sub>O. Some studies have reported the general assistant role from the added Pd in dissociating molecular H<sub>2</sub>, which could enhance the hydrogenation activity for some reactions, such as methanol synthesis<sup>23</sup> and alkynes hydrogenation.<sup>24</sup> Therefore, the promoted activity of 0.1Pd/Cu-fiber is likely attributed to the assistant dissociation of H<sub>2</sub> on Pd sites with spillover of active H species onto the neighboring Cu<sup>+</sup> sites where DMO hydrogenolysis takes place. However, simultaneously with promoting the hydrogenolysis of DMO, such assistant role of Pd visibly facilitates the reduction of Cu<sub>2</sub>O (*i.e.*, the aforementioned crucial catalytic active sites of Cu<sup>+</sup> for the hydrogenolysis of DMO<sup>2,13,21,22</sup>) thereby leading to a very short lifetime of 0.1Pd/Cu-fiber (Fig. S5b). Interestingly, TPR profiles show that the reduction of Cu<sub>2</sub>O-CuO is delayed to 495 °C for the 0.5Au/Cu-fiber (Fig. S4), much higher than that for the 0.1Pd/Cu-fiber and Cu-fiber (Fig. 2a). The delayed reduction of cationic Cu over 0.5Au/Cu-fiber should be attributed to the stabilizing-effect of Au on cationic Cu.<sup>3,14</sup> Accordingly, we believe that the introduction of Au is beneficial for modifying the metallic-Cu/cationic-Cu proportion to a proper level and assuring its maintenance, which improves the catalyst activity,<sup>14</sup> and enhances the catalyst stability (Fig. S5). For the 0.1Pd-0.5Au/Cu-fiber, interestingly, adding Pd does not cause a decrease of the reduction temperature (535 °C) of cationic Cu (Fig. S4, Fig. 2a) compared to the 0.5Au/Cu-fiber catalyst. This indicates that Au-Pd shows strong stabilizing effect on cationic Cu like Au alone, being consistent with good stability of 0.1Pd-0.5Au/Cu-fiber among these catalysts (Fig. 1d and S5).

In order to further reveal the multi-synergistic nature of the Pd-Au-Cu<sup>+</sup> ternary complex, the samples reacting at different stages in the stability-testing process are collected for every catalyst (Cu-fiber, 0.1Pd/Cu-fiber, 0.5Au/Cu-fiber, and 0.1Pd-0.5Au/Cu-fiber). The collected samples are all characterized by X-ray photoelectron spectroscopy (XPS), indicating that the chemical state of Cu exhibits an interesting evolution in this process on these catalysts (Fig. 2b,c). Because Cu 2p<sub>3/2</sub> XPS cannot differentiate between Cu<sup>+</sup> and Cu<sup>0</sup>, Auger Cu LMM spectra are recorded to confirm the presence of Cu<sup>+</sup> at BE (binding energy) 570.0 eV and Cu<sup>0</sup> at BE 567.7 eV.<sup>25-27</sup> For the pure Cu-fiber, the Cu<sup>+</sup> fraction is 70.6% over the working sample after 10 h running, but decreases to 43% after 30 h running with DMO conversion

decreased from 40% to 12% (Fig. 2b, Table S5, Fig. S5a). For the 0.1Pd/Cu-fiber, the Cu<sup>+</sup> fraction decreases from 55% to 34% with the running time from 10 h to 50 h and DMO conversion from 98% to 42% (Fig. 2b, Table S5, Fig. S5b). In contrast, Cu<sup>+</sup> fraction over the 0.5Au/Cu-fiber catalyst could remain at 63-65% in the 60 h running on-stream (Fig. 2c, Table S5) with a steady DMO conversion of 90-92% (Fig. S5c). Analogously, the Cu<sup>+</sup> fraction over 0.1Pd-0.5Au/Cu-fiber also remains at 62-63% in the 60 h running on-stream (Fig. 2c, Table S5), delivering 99% conversion even after 200 h running, Fig. 1d). These results unanimously indicate the crucial role of Cu<sup>+</sup> in the DMO hydrogenolysis according to the corresponding conversion decline associated with the decrease of Cu<sup>+</sup> fraction. Pd shows ability to promote the catalytic activity (TOF: 80 h<sup>-1</sup> for 0.1Pd/Cu-fiber vs. 17 h<sup>-1</sup> for Cu-fiber, in Table 1) but not the stability because of a fast reduction of Cu<sup>+</sup> to Cu<sup>0</sup>. Au provides dual activity/stability-promoting effect, clearly observed over the 0.5Au/Cu-fiber. Interestingly, with the addition of Pd into 0.5Au/Cu-fiber, the catalyst activity (TOF: 612 h<sup>-1</sup> for 0.1Pd-0.5Au/Cu-fiber vs. 174 h<sup>-1</sup> for 0.5Au/Cu-fiber, in Table 1) is dramatically enhanced again but not deteriorates the catalyst stability, predicting some special synergistic effect between Pd and Au which significantly improves the activity of Cu<sup>+</sup> but not attenuates the ability of Au for stabilizing Cu<sup>+</sup> sites.

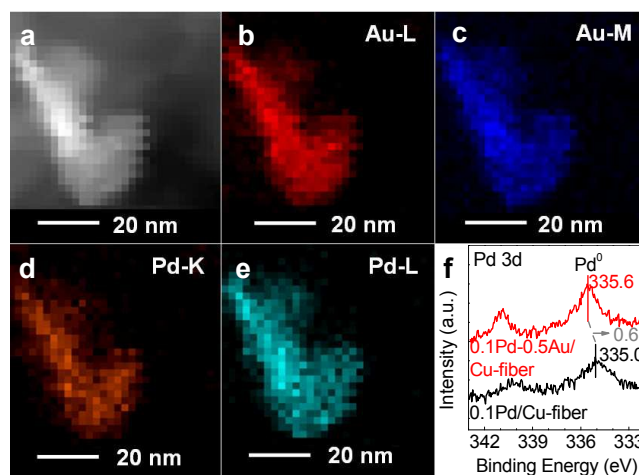
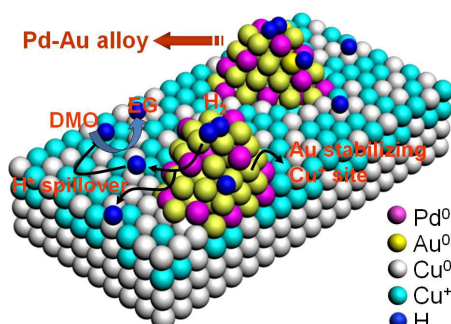


**Fig. 3** (a) HAADF-STEM image. (b-e) The corresponding elemental maps. (f) XPS spectra of Pd 3d of the used 0.1Pd/Cu-fiber and 0.1Pd-0.5Au/Cu-fiber.

The TPR experiments for the Pd-Au/Cu-fiber catalysts with 0.5 wt% Pd but varied Au/Pd weight ratio were carried out, showing without suspense that the reduction temperature of the cationic Cu species is delayed to 460 °C even with a very low Au/Pd ratio of 1/5, and progressively to 575 °C when increasing the Au/Pd ratio to 5/1 (Fig. S6). This further confirms the strong stabilizing-effect of Au on the Cu<sup>+</sup> species even when adding Pd. However, a question naturally arises as to what happened with respect to nanostructure and electron interaction for Au and Pd in the Pd-Au-Cu<sup>+</sup> ternary complex. To seek the answer, the 0.1Pd-0.5Au/Cu-fiber catalyst (after reaction for 10 h) was characterized by transmission electron microscopy (TEM), showing the Pd-Au NPs with unique size of 4±1 nm (Fig. S3a). The corresponding elemental maps of high angle annular dark-field scanning transmission electron microscopy (HAADF-STEM) micrograph further show that Pd distributes homogeneously with Au in the

mapped part (Figs 3a-3e), indicating the formation of Au-Pd alloy. As previously noted, Au@Pd core-shell and Au-Pd alloy all deliver alike strong electron interaction.<sup>28-31</sup> Indeed, the XPS results for the 0.1Pd-0.5Au/Cu-fiber catalyst (after reaction for 10 h) show an obvious up-shifting of the metallic Pd 3d<sub>3/2</sub> BE from 335.0 eV for 0.1Pd/Cu-fiber to 335.6 eV for 0.1Pd-0.5Au/Cu-fiber (Fig. 3f), while a slight down-shifting of the metallic Au 4f<sub>7/2</sub> BE is observed from 84.2 eV for 0.5Au/Cu-fiber to 84.0 eV for 0.1Pd-0.5Au/Cu-fiber (Fig. S7, likely due to the low Pd/Au weight ratio of only 1/5). The results indicate that Pd species for the 0.1Pd-0.5Au/Cu-fiber is electron deficient to some extent because of the Au electron-drawing effect, which is originated from the Pd-Au electron interaction, and moreover, is observed in both Au@Pd core-shell and Au-Pd alloy nanostructure.<sup>29-31</sup> For another important reaction of the direct synthesis of H<sub>2</sub>O<sub>2</sub> from H<sub>2</sub> and O<sub>2</sub>, which also involves the H<sub>2</sub>-converting, such electron interaction delivers much higher H<sub>2</sub> conversion than either Pd or Au, because of the improved ability for H<sub>2</sub> activation to generate more active hydrogen species.<sup>29-31</sup> We thus tentatively infer that dramatic improvement of the DMO hydrogenolysis activity for the 0.1Pd-0.5Au/Cu-fiber catalyst, by analogy with Au@Pd core-shell composite and Au-Pd alloy for direct H<sub>2</sub>O<sub>2</sub> synthesis,<sup>29-31</sup> is also likely due to the Pd-Au electron interaction in Au-Pd alloy. In addition, such electron interaction between Au and Pd also plays a key role likely in suppressing Pd-catalyzed reduction of the cationic Cu species thereby assuring the stability maintenance.



**Scheme 1.** The illustration of proposed ternary Pd-Au-Cu<sup>+</sup> complex for DMO hydrogenolysis to EG.

In summary, our results establish that structured Pd-Au/Cu-fiber with 0.1 wt% Pd and 0.5 wt% Au is a promising catalyst for the gas-phase hydrogenolysis of DMO to EG, and it is active, selective, stable and highly thermal conductive. The Pd and Au can be embedded into the Cu-fiber through one-step facile galvanic deposition method. A ternary Pd-Au-Cu<sup>+</sup> complex is tentatively proposed as illustrated in Scheme 1, in which Cu<sup>+</sup> acts as an essential site for the gas-phase DMO hydrogenolysis, and Au-Pd alloy synergistically promotes the hydrogenolysis activity of Cu<sup>+</sup> sites as a result of strong Au-Pd electron interaction while Au plays a key role in stabilizing Cu<sup>+</sup> sites to prevent deep reduction deactivation especially the Pd-catalyzed reduction. We anticipate that our finding will initiate the attempts to develop the microstructured catalyst, and more importantly, to inspire the research activities concerning in-depth understanding of the synergistic-promotion-effect stemmed from Pd-Au-Cu<sup>+</sup> complex for the DMO hydrogenolysis and other related processes.

This work was funded by the “973 program” (2011CB201403) from the MOST of China and the NSF of China (21473057, 21273075, U1462129, 21076083).

## Notes and references

Shanghai Key Laboratory of Green Chemistry and Chemical Processes, School of Chemistry and Molecular Engineering, East China Normal University, Shanghai 200062, China. E-mail: ylu@chem.ecnu.edu.cn; gzhao@chem.ecnu.edu.cn.

<sup>†</sup>Electronic Supplementary Information (ESI) available: Experimental and TOF calculations details; characterizations of the prepared catalysts and test results over the reference catalysts. See DOI: 10.1039/b000000x/  
<sup>‡</sup> These authors contributed equally to this work.

- 1 A. Corma, S. Iborra and A. Velty, *Chem. Rev.* 2007, **107**, 2411.
- 2 J. Gong, H. Yue, Y. Zhao, S. Zhao, L. Zhao, J. Lv, S. Wang and X. Ma, *J. Am. Chem. Soc.* 2012, **134**, 13922.
- 3 P. Liu and E. J. M. Hensen, *J. Am. Chem. Soc.* 2013, **135**, 14032.
- 4 J. W. van Hal, J. S. Ledford and X. K. Zhang, *Catal. Today.* 2007, **123**, 310.
- 5 R. A. Kerr and R. F. Service, *Science* 2005, **309**, 101.
- 6 Z. N. Xu, J. Sun, C. S. Lin, X. M. Jiang, Q. S. Chen, S. Y. Peng, M. S. Wang and G. C. Guo, *ACS Catal.* 2013, **3**, 118.
- 7 H. T. Teunissen and C. J. Elsevier, *Chem. Commun.* 1997, 667.
- 8 Y. Zhu, S. Wang, L. Zhu, X. Ge, X. Li and Z. Luo, *Catal. Lett.* 2010, **135**, 275.
- 9 H. Yue, Y. Zhao, X. Ma and J. Gong, *Chem. Soc. Rev.* 2012, **41**, 4218.
- 10 X. Zheng, H. Lin, J. Zheng, X. Duan and Y. Yuan, *ACS Catal.* 2013, **3**, 2738.
- 11 C. Wen, Y. Cui, W. Dai and K. Fan, *ChemCatChem* 2013, **5**, 138.
- 12 D. J. Thomas, J. T. Wehrli, M. S. Wainwright and D. L. Trimm, *Appl. Catal. A* 1992, **86**, 101.
- 13 Z. He, H. Lin, P. He and Y. Yuan, *J. Catal.* 2011, **277**, 54.
- 14 Y. Wang, X. Duan, J. Zheng, H. Lin, Y. Yuan, H. Ariga, S. Takakusagi and K. Asakura, *Catal. Sci. Technol.* 2012, **2**, 1637.
- 15 C. Wen, Y. Cui, X. Chen, B. Zong and W. L. Dai, *Appl. Catal. B* 2015, **162**, 483.
- 16 C. Wen, Y. Cui, W. L. Dai, S. Xie and K. Fan, *Chem. Commun.* 2013, **47**, 5195.
- 17 H. Yue, Y. Zhao, L. Zhao, J. Lv, S. Wang, J. Gong and X. Ma, *AIChE J.* 2012, **58**, 2798.
- 18 A. Yin, X. Guo, W. Dai and K. Fan, *Appl. Catal. A* 2008, **349**, 91.
- 19 G. Zhao, M. Deng, M. Ling and Y. Lu, *Green Chem.* 2011, **13**, 55.
- 20 G. Zhao, Y. Li, Q. Zhang, M. Deng, F. Cao and Y. Lu, *AIChE J.* 2014, **60**, 1045.
- 21 D. Brands, E. Poels and A. Bliet, *Appl. Catal. A* 1999, **184**, 279.
- 22 E. K. Poels and D. S. Brands, *Appl. Catal. A* 2000, **191**, 83.
- 23 I. Melián-Cabrera, M. L. Granados and J. L. G. Fierro, *J. Catal.* 2002, **210**, 285.
- 24 A. J. McCuea, C. J. McRitchiea, A. M. Shepherd and J. A. Anderson, *J. Catal.* 2014, **319**, 127.
- 25 K. L. Deutsch and B. H. Shanks, *J. Catal.* 2012, **285**, 235.
- 26 F. Severino, J. L. Brito, J. Laine, J. L. G. Fierro and A. L. Agudo, *J. Catal.* 1998, **177**, 82.
- 27 I. Platzman, R. Brener, H. Haick and R. Tannenbaum, *J. Phys. Chem. C* 2008, **112**, 1101.
- 28 D. I. Enache, J. K. Edwards, P. Landon, B. Solsona-Espriu, A. F. Carley, A. A. Herzing, M. Watanabe, C. J. Kiely, D. W. Knight and G. J. Hutchings, *Science*, 2006, **311**, 362.
- 29 J. K. Edwards, S. J. Freakley, A. F. Carley, C. J. Kiely and G. J. Hutchings, *Acc. Chem. Res.* 2013, **47**, 845.
- 30 J. K. Edwards, B. E. Solsona, P. Landon, A. F. Carley, A. Herzing, C. J. Kiely and G. J. Hutchings, *J. Catal.* 2005, **236**, 69.
- 31 J. K. Edwards, A. Thomas, A. F. Carley, A. A. Herzing, C. J. Kiely and G. J. Hutchings, *Green Chem.* 2008, **10**, 388.